WIRE-MESH SENSORS FOR HIGH-RESOLUTION GAS-LIQUID MULTIPHASE FLOW VISUALIZATION

Marco Jose da Silva, m.dasilva@fzd.de
Sebastian Thiele, s.thiele@fzd.de
Eckhard Schleicher, e.schleicher@fzd.de
Uwe Hampel, u.hampel@fzd.de
Institute of Safety Research, Forschungszentrum Dresden-Rossendorf, Bautzner Landstrasse 400, 01328 Dresden, Germany

Abstract. *Wire-mesh sensors are flow imaging devices and allow the investigation of multiphase flows with high spatial and temporal resolution. This type of sensor was introduced about ten years ago at Research Center Dresden-Rossendorf, Germany and since then it has been successfully employed to investigate several single phase and two-phase flow phenomena. The sensor can be seen as a hybrid solution in between intrusive local measurement of phase fraction and tomographic cross-sectional imaging. It comprises of two set of wires stretched over the cross-section of a vessel or pipe. The planes of wires are perpendicular to each other with a small axial separation between them, thus forming a grid of electrodes. The associated electronics measures an electrical property of the flowing media at each crossing point in a very fast and multiplexed manner. The wire mesh subdivides the flow channel cross section into a number of independent sub-regions, whereas each crossing point represents one sub-region. Each of the measured signals reflects the constitution of the flow within its associated sub-region, i.e. each crossing point acts as local phase indicator. Hence, the set of data obtained from the sensor directly represents the phase distribution over the cross-section and no reconstruction procedure, e.g. by solving an inverse problem as usual in tomography, is needed in order to determine cross-sectional phase distributions. The first generation of wire-mesh sensors is based on conductivity measurements, thus being able to investigate electrically conducting fluids only. Typically air-water and steam-water flows have been investigated. Recently, the capacitance wire-mesh sensor has been developed and tested, which allow the investigation of non-conducting fluids such as oil or organic liquids. The newest systems are able to produce up to 10,000 images per second. Sensors can be constructed to operate under temperatures up to 286 °C and pressures up to 7 MPa. First this article reviews the measuring principle of wire-mesh sensors. In addition, measurement results of the application of a new-developed capacitance wire-mesh sensor to investigate two-phase gas-oil flow are presented. Furthermore, the use of a wire-mesh sensor for the investigation of a simulated three-phase flow in a laboratory setup is described and discussed. Thus, the wire-mesh sensor can considered as a simpler and inexpensive alternative to investigate either two-phase gas-liquid or three-phase gas-liquid-liquid flows. The good accuracy achieved in the permittivity measurement allows the wire-mesh system to securely distinguish even each of the three phases of a gas-oil-water flow.*

Keywords*: multiphase flow, flow visualization, phase fraction, wire-mesh sensor, imaging system*

1. INTRODUCTION

Multiphase flow denotes the simultaneous stream of two or more physically distinct and immiscible substances. Two-phase gas-liquid flow are among the most import types of multiphase flow and occurs extensively throughout industries, for instance, in boilers, gas and oil transport pipelines, chemical processes. In many applications, such flows determine safety and efficiency of the processes and plants where they occur. Therefore, measurement and imaging of multiphase flows has received much attention in recent years, largely driven by the need of many industry branches to accurately quantify, predict and control the flow of multiphase mixtures. Therefore a considerable number of measuring techniques to investigate multiphase flow have been developed in the past. In addition, measuring techniques are also required for the generation of reliable experimental data which are employed in the validation of computational fluid dynamic (CFD) codes. CFD code validation requires small and medium scale multiphase flow experiments with accurate, multi-dimensional and non- or minimal intrusive measurement techniques for different physical parameters, such as phase fraction distributions, temperature fields, velocity fields, and/or concentration fields. Also therefore, the development of reliable multiphase flow measurement techniques has got a strong impulse in recent years. Good reviews about state-of-the-art measurement techniques for multiphase flow are given for example in Dyakowsky (1996), Bennett et al. (1999), and Boyer et al. (2002).

Opposed to single phase flow, multiphase flows are often not accessible for optical or ultrasound measurement techniques due to the presence of opaque fluids or multiphase flow with high to moderate interfacial area density, and thus techniques such as LDA, PIV, US-Doppler may fail in many practical situations. Tomographic visualization techniques are found to be very attractive to investigate multiphase flow. Tomography can be used to non-invasively visualize flow problems in mechanical or chemical process engineering occurring in pipes, vessels, armatures, machines, and so on. In recent years, mainly two types of flow tomography have been developed and partially qualified for the case of two and multiphase flows, namely electrical tomography techniques and radiation-based tomography

techniques. Examples are electrical impedance, capacitance and resistance tomography (York 2001), x-ray (Hervieu et al. 2002) and gamma ray tomography (Hampel et al. 2007), PET (Parker and McNeil 1996), and MRI (Mantle et al. 2002). Electrical-type tomography techniques are easy to apply, inexpensive and potentially fast. However, they suffer from low spatial resolution which does not enable to measure gas bubble size profiles or interfacial areas exactly. X-ray tomography is able to achieve high resolution and gamma rays can penetrate thick metallic vessel walls and are therefore more suitable for larger vessels. However, gamma and x-ray techniques are slow. Thus, it is only possible to measure stationary flows or time-averaged gas hold-up profiles. Similar limitations are found for PET and MRI systems.

A technique similar to flow tomography is wire mesh sensor imaging. A first simple type of wire-mesh sensor was introduced by Reinicke et al. (1996). Here, pair-wise measurement of conductivity of a three-plane wire-mesh and successive tomographic image reconstruction using iterative inverse algorithms was suggested. However, point-wise wire-mesh sensing, that was proposed by Prasser et al. (1998), first provided artifact-free two-dimensional phase images of gas-liquid flow with unprecedented temporal and spatial resolution and no necessity of solving a highly ill-posed inverse problem. The sensor is a hybrid solution in between invasive local measurement of phase fraction and tomographic cross-sectional imaging. The sensor comprises of two set of wires stretched over the cross-section of a vessel or pipe. The planes of wires are perpendicular to each other, thus forming a grid of electrodes (fig. 1). The associated electronics measures an electrical property of the flowing media at each crossing point. Based on those measurements and knowing a-priori the electrical properties of the substances involved in the flow, the sensor is thus able to determine instantaneous fluid distribution over the cross-section. The first generation of wire-mesh sensors is based on conductivity measurements, thus being able to investigate electrically conducting fluids only. Typically air-water and steam-water flows have been investigated. Recently, the capacitance wire-mesh sensor has been developed and tested, which allow the investigation of non-conducting fluids such as oil or organic liquids (Da Silva et al. 2007).

In this article, first the basic operating principle of wire-mesh sensors is reviewed along with some examples of utilization of such a sensor for the investigation of multiphase flows. Further, the wire-mesh sensor is for the first time applied to investigate a (simulated) three-phase flow in a laboratory setup. Limitations and possibilities are discussed.

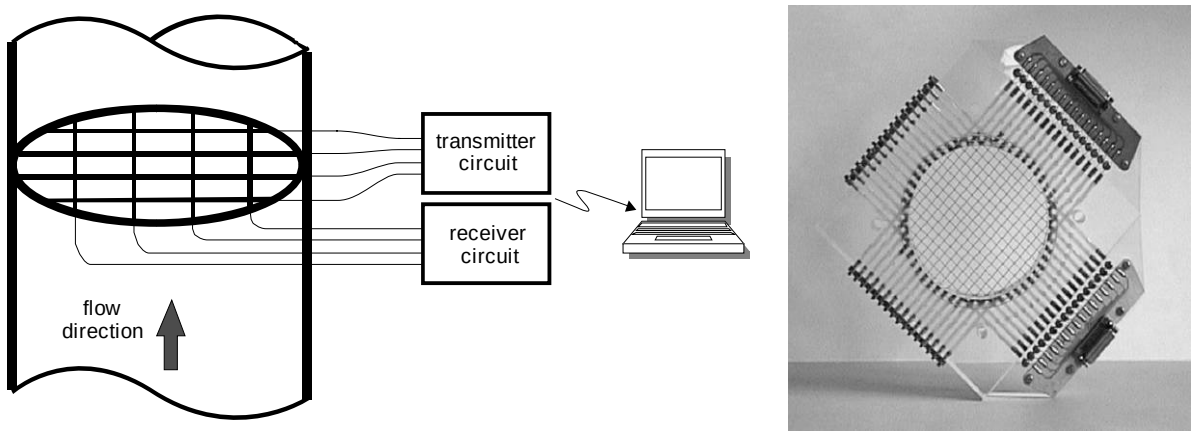

Figure 1: (a) schematic representation of a wire-mesh sensor; (b) photograph of a typical low-pressure sensor developed at FZD.

2. WIRE-MESH SENSORS

2.1 Measuring principle

As already mentioned the basic idea of a wire-mesh sensor is to stretch a set of wires over the cross-section in two adjacent planes whereby wires in each plane run parallel to each other. The wires of the one plane are used as transmitters and the wires of the other plane as receivers. Figure 2a shows the block diagram of the electronics of a capacitance wire-mesh sensor for an exemplary sensor with 4 × 4 wires. The transmitter wires are activated by supplying them with voltage excitation signal in successive order which is controlled by switches S1 to S4 (fig. 2b). The non-activated electrodes are connected to ground potential. The current at a receiver wire resulting from the activation of a given transmitter wire is a measure of the electric permittivity of the fluid in the corresponding control volume close to the crossing point of the two wires. The currents from all receiver wires are sampled simultaneously. This procedure is repeated for all transmitter electrodes being activated once. After activating the last transmitter wire, a complete set of measurements for the whole cross-section has been acquired. The measurements are in fact voltages which are proportional to the electric permittivity of the medium around each crossing point of the wire grid at the very

moment of data sampling. In this manner, the wire mesh subdivides the flow channel cross-section into a number of independent sub-regions, where each crossing points represents one sub-region. Each of the measured signals reflects the constitution of the flow within its associated sub-region, i.e. each crossing point acts as local phase detector. Hence the set of data obtained from the sensor directly represents the phase distribution over the cross-section and no reconstruction procedure, e.g. solving an inverse problem as usual in tomography, is needed in order to determine cross-sectional phase distributions.

For the capacitance measurement, an AC excitation and measuring scheme is used. Therefore a sinusoidally alternating voltage (typically of 5 MHz) is employed for excitation and the receiver circuit must encompass a demodulator which converts the AC voltage into a proportional DC one. The sequential activation scheme for the transmitter wires and the parallel measurement of the receiver currents is the same as for the conductivity electronics. Relative electric permittivity (or dielectric constants) values very close such as for air ($\varepsilon_r = 1$) and oil ($\varepsilon_r \approx 2$) can be securely distinguished by a capacitance wire-mesh sensor (Da Silva et al. 2007).

Over the past ten years FZD has invented, developed and tested wire-mesh sensors for different applications in multiphase flow measurement. From the first publication (Prasser et al. 1998) the technology has steadily been developed towards increasing frame rate (Prasser et al. 2002a), bubble size measurement (Prasser et al. 2001), gas phase velocity measurement (Manera et al. 2006), measurement at elevated pressures (Pietruske and Prasser 2007), measurements under critical operation conditions such as water hammers and cavitation shocks (Dudlik et al. 2002), miniaturization of sensor for the investigation of small pipes (Hampel et al. 2009), and the use of electrical capacitance measurements (Da Silva et al. 2007). Today sensors can be devised with up to 128 × 128 wire configuration, wire diameter down to 50 µm, in diversity of different cross-section geometry and operating parameters. High-pressure wire-mesh sensor can be employed in an environmental conditions range of up to 286 °C and 7 MPa. Associated electronics for signal generation and data acquisition achieves a maximum temporal resolution of 10,000 frames per second.

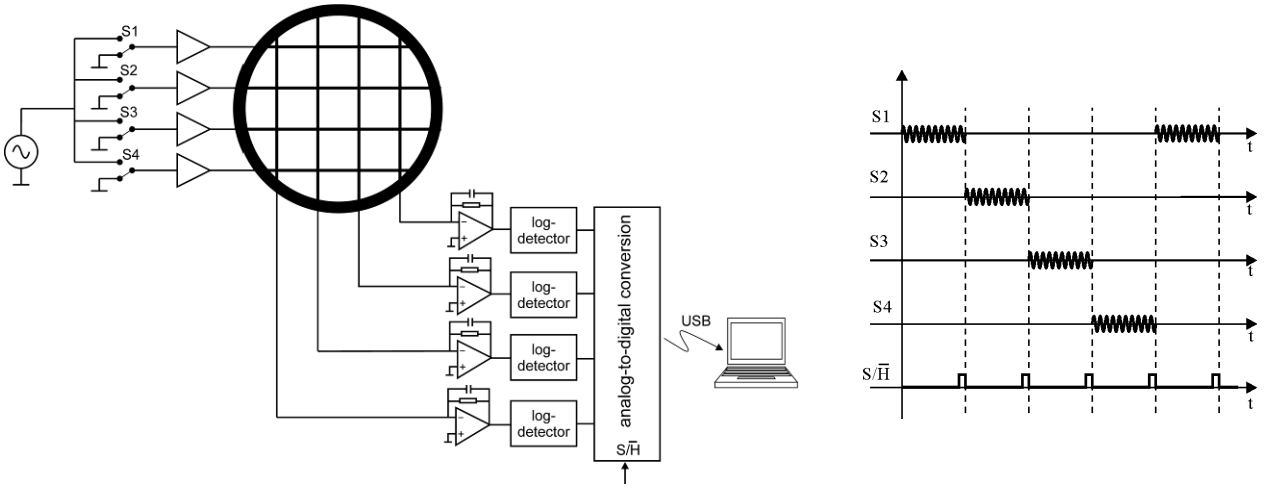

Figure 2: Capacitance wire-mesh sensor electronics with a 4 × 4 electrodes configuration. (a) Block diagram and (b) time diagram for the excitation-probing scheme.

2.1 Void fraction measurement and image processing

In order to discriminate two non-conducting fluids such as air and silicone oil, the capacitance or the permittivity of a crossing point is evaluated. The permittivity-based electronics generates a voltage V proportional to the relative permittivity ε_r of the fluid present at a crossing point according to (Da Silva et al. 2007)

$$V = a \cdot \ln\left(\varepsilon_r\right) + b \tag{1}$$

where a and b are constants that encompass the specific parameters of the electronics. The logarithmic function allows for the measurement of permittivities in a broad range without the need for any adjustment, i.e. in an open-loop approach, thus assuring a fast time response.

Repeated successive activation of all transmitter electrodes and measurement of (displacement) currents for all receiver channels gives a three-dimensional data matrix with electrical voltage values denoted by $V(i,j,k)$ which

corresponds to permittivity distributions over the pipe cross section. Here, *i* and *j* are the spatial indices (corresponding to the wire numbers) and *k* is the temporal index of each image.

Equation (1) hold for every crossing point in the grid of a wire-mesh sensor. It is obvious that the constants in these equations may be different for all the (*i*,*j*) crossing points. Thus, a calibration of these channels is necessary to obtain accurate output readings, which is described as follows. In the calibration routine, first the cross section is filled up with a substance with low permittivity ε_r^L and for this situation a data matrix $V^L(i,j)$ is acquired. Normally average values over a certain time are used to reduce statistical signal fluctuations. In a second situation, the entire cross section is covered with another substance having a higher permittivity ε_r^H and the same procedure is repeated, getting the data matrix $V^H(i,j)$. In this fashion, applying equation (1) for both calibration data matrixes is possible to calculate the constants of (4) as

$$a(i,j) = \frac{V^H(i,j) - V^L(i,j)}{\ln\left(\varepsilon_r^H\right) - \ln\left(\varepsilon_r^L\right)} \tag{2}$$

$$b(i,j) = \frac{V^L(i,j)\ln\left(\varepsilon_r^H\right) - V^H(i,j)\ln\left(\varepsilon_r^L\right)}{\ln\left(\varepsilon_r^H\right) - \ln\left(\varepsilon_r^L\right)} \tag{3}$$

Finally, we can calculate the relative permittivity distribution over the sensor cross section by inverting (1) and applying it for every crossing point, thus

$$\varepsilon_r(i,j) = \exp\left(\frac{V - b(i,j)}{a(i,j)}\right) \tag{4}$$

For the calculation of the local phase fraction distribution $\alpha(i,j)$, a linear relationship between the measured permittivity and the phase fraction is assumed

$$\alpha(i,j,k) = \frac{\varepsilon_r^H - \varepsilon_r(i,j,k)}{\varepsilon_r^H - \varepsilon_r^L} \tag{5}$$

The assumption of a linear dependency between the local phase fraction level and the output voltage (permittivity) is obviously a simplification. For the case of complex multiphase or multi-component flows, more elaborated relationships may be necessary, for instance encompassing models for the effective permittivity of mixtures. This way, (5) can be understood as first order approximation.

From phase fraction distributions, axial and radial gas content profiles as well as the integral gas fraction can be determined by integration of the measured data over appropriate partial volumes. Further data post-processing on matrix $\alpha(i,j,k)$ is then performed to identify single bubbles or determine characteristic bubble or phase boundary parameters (Prasser et al. 2001).

Two visualization techniques are frequently used to show the three-dimensional data $\alpha(i,j,k)$: axial slice images and side projections. In the former one, the temporal evolution of the phase fraction values of only the crossing points along the central electrode is displayed. Thus, such an image has the character of a side view to the flow on a vertical plane cut through the pipe along its vertical axis. With the second technique, side projections are processed using a simplified ray-tracing algorithm as described in detail in Manera et al. (2006). In this visualization technique an illumination of the three-dimensional phase fraction distribution by parallel white light is assumed and the light intensity departing in the direction of a virtual observer is calculated. This method supplies instructive pseudo-3D imaging.

3. EXPERIMENTAL RESULTS

3.1 Two-phase flow measurement

In this section we present an exemplary application of the wire-mesh sensor to investigate a two-phase pipe flow. The measurements were conducted in a test facility of the Chemical Engineering Laboratory of the School of Chemical and Environmental Engineering, University of Nottingham, UK (Hernandez Perez et al. 2007, Thiele et al. 2008). The facility consists of 6 m long 67 mm internal diameter vertical pipe. Inlet volumetric flow rates of liquid phase and air are determined by a set of rotameters. Silicone oil with density of 900 kg/m^3 and viscosity of 5.25 mPa·s was employed as a liquid. The oil is taken from a storage tank and air from the main laboratory compressed-air system. The pipe outlet is connected to a separator where air is released to atmosphere and the oil is returned into the storage tank, thus being circulated in close loop. The wire-mesh sensor was located 5 m from the inlet, i.e. 74.6 pipe diameters. Experiments

were performed at liquid superficial velocities J_L = 0.25 m/s and at gas superficial velocity range (J_G) of 0.06 to 5.56 m/s. The wire-mesh sensor was set up to acquire images of the flow at 5,000 fps during 5 s.

In the images of figure 3 the transition of a few different flow regimes can be visualized with both visualization techniques described in section 2. The gaseous phase is represented by a bright color and the liquid phase by a dark one. At lowest gas flow rates bubbly flow is observed. By increasing the gas superficial velocities the transition to slug flow, churn turbulent flow, and finally to annular flow occurs. The vertical axis represents the time of 5 s.

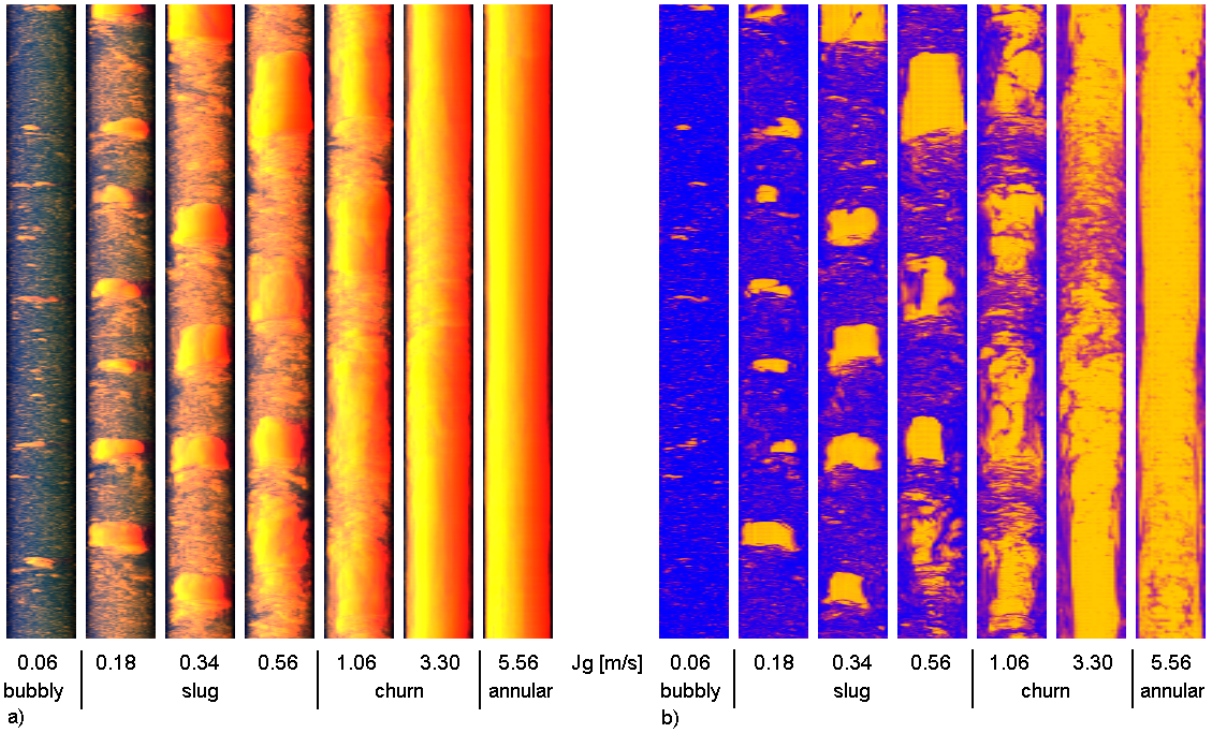

Figure 3: Visualization of wire-mesh sensor data for superficial velocity of silicone oil J_L = 0.25 m/s and different gas superficial velocities; a) side projections; b) axial slice images.

Some quantitative insights of the flow can be obtained by proper integration of the three-dimensional void fraction data α(i,j,k) over appropriated sub-volumes. Thus by integrating the data over circular segments, time-averaged radial profiles can be obtained (Prasser et al. 2002b). Figure 4a shows these profiles for all gas superficial velocities studied here. All peak values are located in the pipe center and increase with increasing gas superficial velocity J_G. The shapes of the curves are developed by appearing of relatively large gaseous structures located in pipe center.

A feature of wire-mesh sensors, which is only possible due to their high spatial and temporal resolution, is the measurement of bubble size distributions. For this purpose, first individual bubbles are indentified with proper image processing algorithms and then their sizes are determined (Prasser et al. 2001). Figure 4b shows bubble size distributions for three selected gas superficial velocities at the investigated superficial liquid velocity of JL= 0.25 m/s. In the figure, the x-axis represents the volume equivalent bubble diameter (Db) and y-axis represents the gas fraction per bubble class ($\Delta\varepsilon$) divided by width of bubble class (ΔDb). For a better visualization the width of bubble classes increase logarithmically. The cases plotted in figure 4b were selected to be in bubbly flow, slug flow and churn flow. It is clear to observe the increase in the bubble sizes with increasing superficial gas velocity. In bubbly flow (J_G = 0.06 m/s) all bubbles are lower than 12 mm. In slug flow (0.56 m/s) bubbles are basically divided into to main peaks, one in the lower range (> 30 mm) and one in the range between 50 and 100 mm, corresponding to the Taylor bubbles. In churn flow (3.30 m/s), the shape of bubble size distribution is similar to slug flow, i.e. the double peak, however size of bubbles tend to be larger and of course the large bubbles are not anymore so well bullet-shaped, as can be seen from fig. 3.

Further quantitative data is obtained by the cross-sectional averaged time series of the void fraction measured by the wire-mesh sensor. For more details in the algorithmic calculation of such time series see Prasser et al. (2002b). Examples of time series are illustrated in fig. 4. The cases were selected to be again in bubbly flow (J_G = 0.06 m/s), slug flow (0.34 m/s) and churn flow (1.06 m/s). The low gas flow rate condition is characterized by low void fraction with quite regular peaks of higher void fraction probably representing clusters of bubbles. The slug flow data has alternate periods of high and low void fraction. The case for higher flow rate is churn flow which has mainly high void fractions with regular troughs of lower signal. In Figure 4 the probably density functions (PDF) of the time series are also plotted,

showing the typical low void fraction peak for bubbly flow, the double peak for slug flow, and the broadened peak at higher void fractions for the churn flow (Costigan and Whalley 1997).

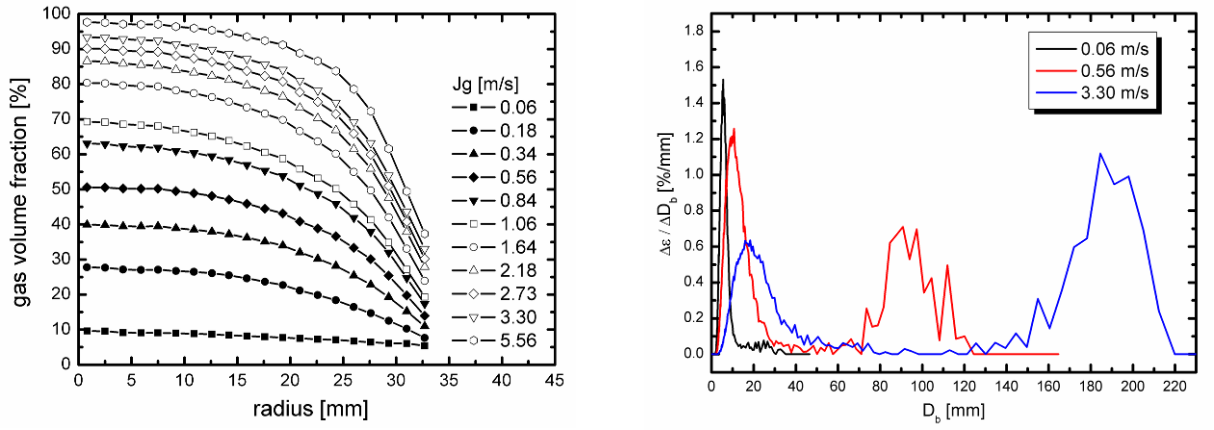

(a) (b)

Figure 4: Radial gas void fraction profiles (a) and bubble size distributions (b) for selected gas superficial velocities JG (indicated in the legend).

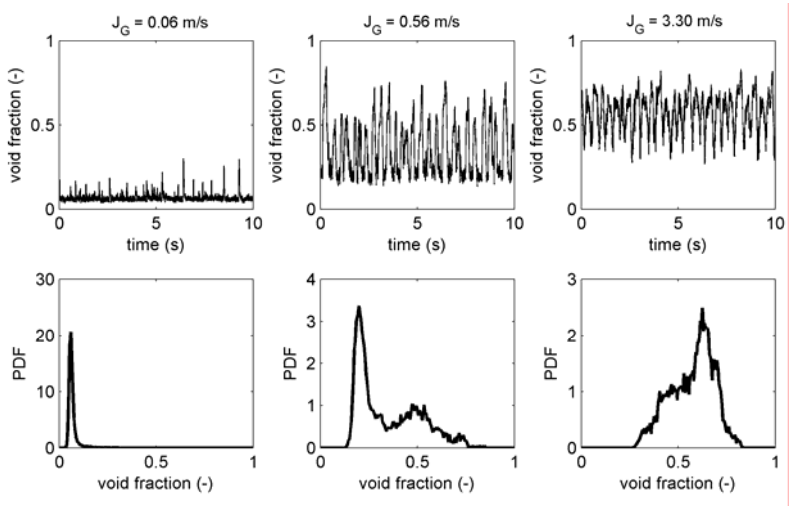

Figure 5: Time series and probably density functions (PDF) of the cross-sectional averaged data for three flow conditions; bubbly (left), slug (middle) and churn flow (right).

3.2 Three-phase flow measurement

Three-phase gas-oil-water flow is a common occurrence in the petroleum industry. Although many different three-phase metering systems have been developed and tested, none can be referred to as generally applicable or universally accurate. Many current systems utilize radioactive sources in their measurement concept, so that such meters must comply with high security and reliability standards due to environmental and legal issues (Corneliussen et al. 2005). Therefore, there is a continuous search for new technologies which may substitute the radiation-based phase fractions measurement.

A possible alternative to the current-in-use systems can be the newly developed capacitance wire-mesh sensor. The good accuracy achieved in the permittivity measurement (Da Silva et al. 2007) allows the wire-mesh system to securely distinguish each of the three phases of an air, oil and water flow. A preliminary test has been performed regarding the capability of the system to investigate a three-phase flow.

In this study we used a laboratory wire-mesh sensor with rectangular section of 50 mm x 50 mm (fig. 6). The sensor is made of two layers with 16 stainless steel wires (diameter 0.12 mm) having 1.5 mm axial plane distance. The

distance between the wires in one layer is 3.12 mm. The wires are mounted in a rectangular acrylic frame that itself is part of a rectangular flow channel.

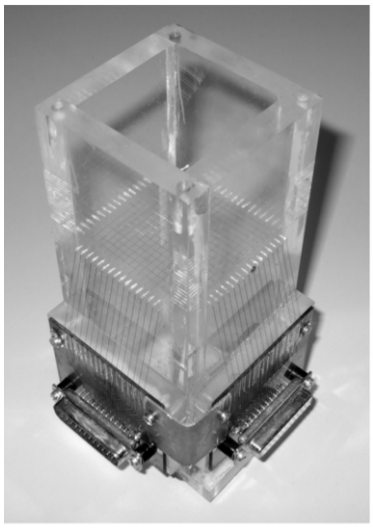

Figure 6: Photograph of the experimental 16 × 16 wire-mesh sensor used for the investigation of three-phase flow.

The flow channel with integrated wire-mesh sensor was filled up with air, oil and water in such a way that each of these substances occupies one third of the cross-section area. It was also placed in a horizontal position. In this way, a three-layer structure as shown in fig. 7 was obtained which imitates a stratified flow. Prior to begin of the experiment a two-point calibration was realized with air and water as reference. One single image was acquired and fig. 7 depicts the result, in which a logarithmic color scale was used for the permittivity values. Although the permittivity values of air ($\varepsilon_r = 1$), oil ($\varepsilon_r = 2$) and water ($\varepsilon_r = 80$) lay in a high dynamic range, all three phases can be clearly recognized.

In order to further investigate the capability of the wire-mesh sensor for investigating transient three-phase flow, the flow channel with integrated sensor, having the three substances air, oil and water, was shaken to simulate a flow in the sensor box. The 16 × 16 wire-mesh sensor was configured to acquire 625 fps while the sensor box was agitated. Figure 8 depicts the slice image for the central electrode of the flow measured during three seconds. With the employed color scale, air is shown in red, oil in orange and water in blue color, respectively. Starting from the stratified condition at the beginning of the experiment, an oil slug followed by two water slugs can be clearly seen. The interfacial areas between each phase are also visible having intermediate colors.

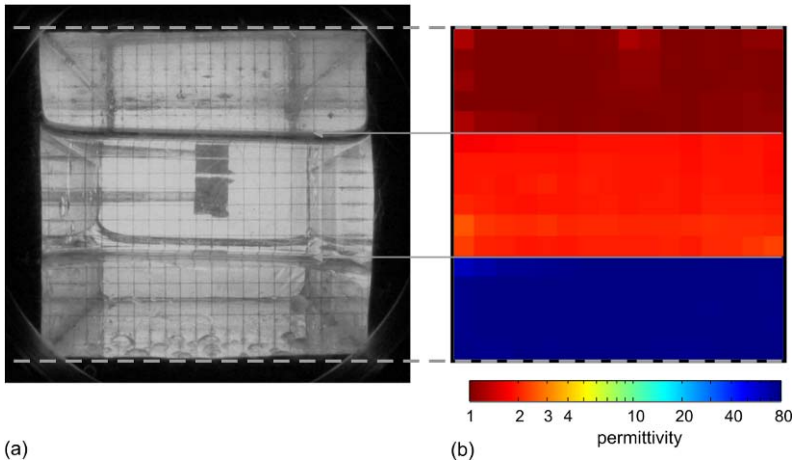

Figure 7: (a) Photo and (b) cross-sectional image of an imitated three-phase stratified flow constituted of air, oil and water. A logarithmic color scale was used for the permittivity values.

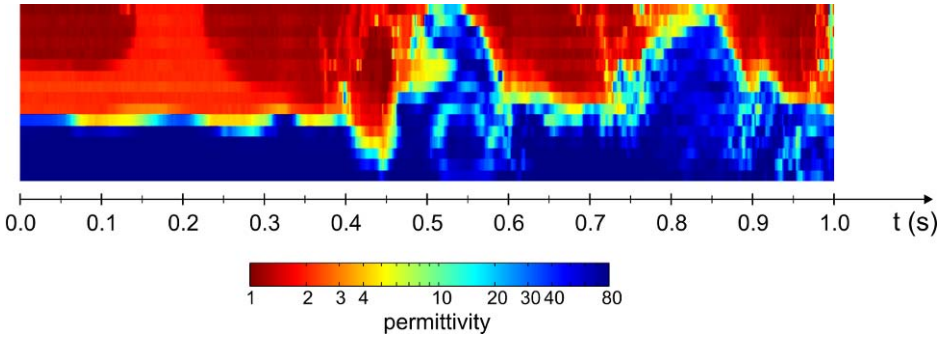

Figure 8: Slice image for the central electrode of the three-phase flow.

A last experiment was carried out aiming to monitor the separation process of a three-phase air-oil-water mixture. For this reason, the sensor box (as previously used) containing the three substances was heftily agitated in order to properly homogenize the multiphase mixture. As a result of the mixing process, an emulsion is formed which was also visually observed. After the agitation the sensor was put at rest. The agitation and the following separation process were monitored by the wire-mesh sensor and in parallel with a video camera. Figure 9 depicts the process evolution where a slice image of the central electrode for a period of 60 s is displayed. The gaseous phase separates very rapidly from the liquid mixture due to the large difference in density between gas and liquid. The emulsion formed by the agitation can be clearly observed as light blue region in the axial view having a permittivity value between 2 (for oil) and 80 (for water). The emulsion is continuously broken up and at the end of the 50 s period the three phases are completely separated. This behavior was also monitored by the video camera. The three snapshots images from the video camera at exemplary time steps (fig. 8a) also show the evolution of the separation process. The emulsion is seen as opaque region due to high light scattering.

The simple experiments described in this section have shown promising results in the investigation of three-phase flow problems, thus encouraging for the further investigation of the performance of the wire-mesh sensor in real three-phase flows.

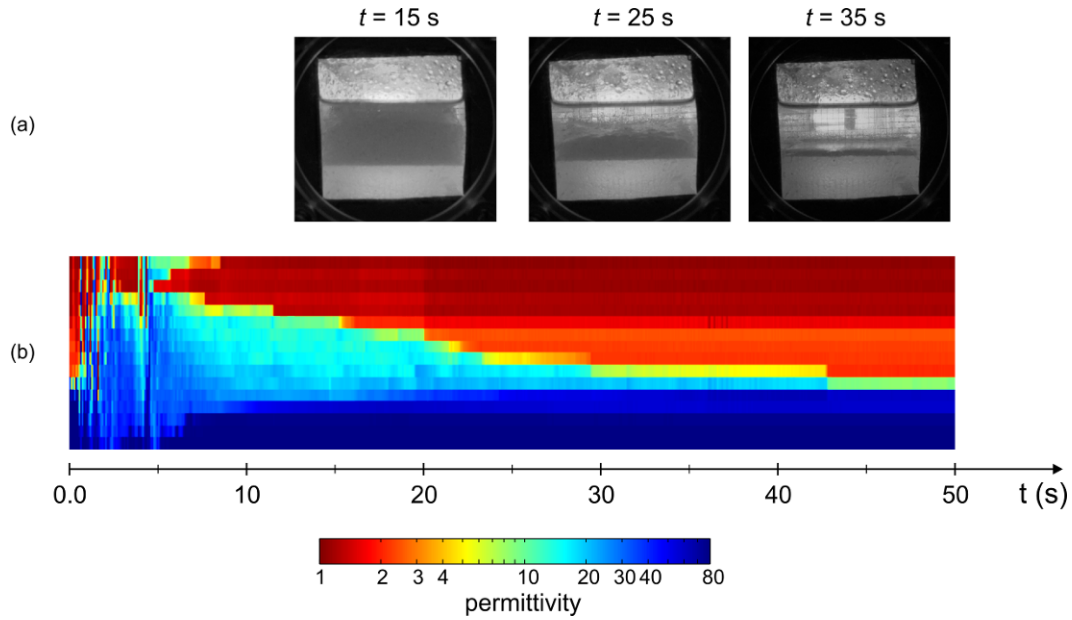

Figure 9: Measurement of the separation process of an air-oil-water mixture. (a) Snapshot images from a video camera and (b) slice image for the central electrode.

4. CONCLUSIONS

Wire-mesh sensors allow the visualization of phase fraction distributions in a high degree of detail due their high spatial and temporal resolution. In this article, a new-developed capacitance wire-mesh sensor was employed to

investigate the two-phase flow of gas and silicone oil in a vertical pipe under industrial conditions. Furthermore, the good system accuracy also allows for the investigation of three-phase air-oil-water mixtures. In preliminary experiments, the three phases in a stratified condition as well as in a simulated flow were correctly acquired, and the emulsion formation was also properly captured by the sensor. The simulated three-phase flow studied here with the sensor can be classified as separated flow. For this type of flow the sensor produced satisfactory results. However, for dispersed flow, where the phases are not anymore readily identifiable, the applicability of sensor will be limited, since the sensor is measuring only one parameter and should identify three different phases. Thus, the evaluation of performance and limitations of the sensor for three-phase flow applications must still be deepener investigated in the future. Nonetheless, the unique features showed in this article make wire-mesh sensors a suitable new tool to investigate dynamic phenomena in multiphase flow.

5. REFERENCES

Bennett M. A., West R. M., Luke S. P., Jia X., Williams R. A. (1999) "Measurement and analysis of flows in a gas-liquid column reactor", Chemical Engineering Science Vol. 54, pp. 5003-5012.

Boyer C., Duquenne A.-M., Wild G. (2002) "Measuring techniques in gas–liquid and gas–liquid–solid reactors", Chemical Engineering Science Vol. 57 pp. 3185-3215.

Corneliussen S., Couput J.-P., Dahl E., Dykesteen E., Frøysa K.-E., Malde E., Moestue H., Moksnes P., Scheers L., and Tunheim H. (2005) Handbook of Multiphase Flow Metering, Rev.2, The Norwegian Society for Oil and Gas Measurement and The Norwegian Society of Chartered Technical and Scientific Professionals. Available at: <http://www.nfogm.no>.

Costigan G., and Whalley P.B. (1997) "Slug flow regime identification from dynamic void fraction measurements in vertical air-water flows", International Journal of Multiphase Flow 23 263-282.

Da Silva M.J., Schleicher E., and Hampel U. (2007) "Capacitance wire-mesh sensor for fast measurement of phase fraction distributions", Measurement Science and Technology Vol. 18, pp. 2245-2251.

Dudlik A., Schönfeld S.B.H., Schlüter S., Fahlenkamp H., and Prasser H.-M. (2002) "Prevention of water hammer and cavitational hammer in pipeline systems", Chemical Engineering and Technology Vol. 2, pp. 888-890.

Dyakowski T. (1996) "Process tomography applied to multi-phase flow measurement", Measurement Science and Technology Vol. 7, pp. 343-353.

Hampel U., Bieberle A., Hoppe D., Kronenberg J., Schleicher E., Sühnel T., Zimmermann W., Zippe C. (2007) "High resolution gamma ray tomography scanner for flow measurement and non-destructive testing applications", Review of Scientific Instruments Vol. 78, pp. 103704.

Hampel U., Otahal J., Boden S., Beyer M., Schleicher E., Zimmermann W., Jicha M. (2009) "Miniature conductivity wire-mesh sensor for gas-liquid two-phase flow measurement", Flow Measurement and Instrumentation Vo. 20, pp. 15-21.

Hernandez Perez V., Azzopardi B.J., and Morvan H. (2007) "Slug flow in inclined pipes", In: Proceedings of 6th International Conference on Multiphase Flow 2007, Leipzig, Germany, July 9 – 13, 2007, Paper No. S5_Thu_C_53.

Hervieu E., Jouet E., Desbat L. (2002) "Development and validation of an x-ray tomograph for two-phase flow", Annals of the New York Academy of Sciences Vol. 972, pp. 87–94.

Manera A, Prasser H.-M, Lucas D., and van der Hagen T.H.J.J. (2006) "Three-dimensional flow pattern visualization and bubble size distributions in stationary and transient upward flashing flow", International Journal of Multiphase Flow Vol. 32, pp. 996-1016.

Mantle M. D., Sederman A. J., Gladden L. F., Raymahasay S., Winterbottom J. M., Stitt E. H. (2002) "Dynamic MRI visualization of two-phase flow in a ceramic monolith", AIChE Journal Vol. 48, pp. 909-912.

Parker D.J. and McNeil P.A. (1996) "Positron emission tomography for process applications", Measurement Science and Technology Vol. 7, pp. 287–296.

Pietruske H. and Prasser, H.-M. (2007) "Wire-mesh sensors for high-resolving two-phase flow studies at high pressures and temperatures", Flow Measurement and Instrumentation Vol.18, pp. 87-94.

Prasser H.-M., Böttger A., and Zschau J. (1998) "A new electrode-mesh tomograph for gas-liquid flows", Flow Measurement and Instrumentation Vol. 9, pp. 111-119.

Prasser H.-M., Scholz D., and Zippe C. (2001) "Bubble size measurement using wire-mesh sensors", Flow Measurement and Instrumentation Vol. 12, pp. 299-312.

Prasser H.-M., Zschau J., Peters D., Pietzsch G., Taubert W., and Trepte M. (2002a) "Fast wire-mesh sensors for gas–liquid flows visualization with up to 10 000 frames per second", In: Proc. Int. Congr. on Advanced Nuclear Power Plants, Hollywood, USA, 2002. Paper #1055.

Prasser H..M., Krepper E., Lucas D. (2002b) "Evolution of the two-phase flow in a vertical tube - decomposition of gas fraction profiles according to bubble size classes using wire-mesh sensors", International Journal of Thermal Sciences Vol. 41, pp. 17–28.

Reinecke N., Boddem M., Petritsch G., Mewes D. (1996) "Tomographisches Messen der relativen Phasenanteile in zweiphasigen Strömungen fluider Phasen", Chemie Ingenieur Technik Vol. 68, pp. 1404-1412.
Thiele S., Da Silva M. J., Hampel U., Abdulkareem L., Azzopardi B. J. (2008) "High-resolution oil-gas two-phase flow measurement with a new capacitance wire-mesh tomograph", In: Proc. 5th International Symposium on Process Tomography In Poland, Zakopane, August 25-26, 2008.
York T.A. (2001) "Status of electrical tomography in industrial applications", Journal of Electronic Imaging Vol. 10, pp. 608-619.

6. RESPONSIBILITY NOTICE

The authors are the only responsible for the printed material included in this paper.